Journal of Physics: Conference Series **628** (2015) 012121 doi:10.1088/1742-6596/628/1/012121

Damage localization by statistical evaluation of signal-processed mode shapes

M.D. Ulriksen and L. Damkilde

Dept. of Civil Engineering, Aalborg University, Niels Bohrs Vej 8, Esbjerg, Denmark

E-mail: mdu@civil.aau.dk, lda@civil.aau.dk

Abstract. Due to their inherent ability to provide structural information on a local level, mode shapes and their derivatives are utilized extensively for structural damage identification. Typically, more or less advanced mathematical methods are implemented to identify damage-induced discontinuities in the spatial mode shape signals, hereby potentially facilitating damage detection and/or localization. However, by being based on distinguishing damage-induced discontinuities from other signal irregularities, an intrinsic deficiency in these methods is the high sensitivity towards measurement noise. The present article introduces a damage localization method which, compared to the conventional mode shape-based methods, has greatly enhanced robustness towards measurement noise. The method is based on signal processing of spatial mode shapes by means of continuous wavelet transformation (CWT) and subsequent application of a generalized discrete Teager-Kaiser energy operator (GDTKEO) to identify damage-induced mode shape discontinuities. In order to evaluate whether the identified discontinuities are in fact damage-induced, outlier analysis of principal components of the signal-processed mode shapes is conducted on the basis of T^2-statistics. The proposed method is demonstrated in the context of analytical work with a free-vibrating Euler-Bernoulli beam under noisy conditions.

1. Introduction

Numerous vibration-based structural health monitoring (SHM) methods have been proposed for damage detection and/or localization of structural damages in aerospace, civil, and mechanical systems, see, e.g., [1, 2, 3, 4]. The applicability of the proposed methods has primarily been tested on the basis of analytical models, finite element (FE) simulations, and controlled laboratory tests; all in which significant simplifications and idealizations are made with regard to, among other things, environmental effects. In this context, it is has been found that the simple methods directly comparing pre- and post-damage vibration-based quantities, such as modal parameters, exhibit only limited potential for damage detection and/or localization, see, e.g., [1, 5]. Under more realistic conditions, these methods turn out to be entirely inapplicable because the direct changes of the aforementioned quantities typically will be concealed by environmental effects and noise contamination. As an example, it is documented in [6, 7] how environmental effects and general operational conditions can account for up to at least 5 % shifts in eigenfrequencies, which, as documented in, e.g., [7, 8], hardly will be exceeded by damage-induced eigenfrequency changes.

As a consequence of the general inadequacy of the simple methods, current research within the field of vibration-based SHM is mainly leveled at developing more sophisticated and robust methods. Some of these methods are based on signal processing of spatial mode shapes signals, which seems auspicious as this modal parameter, contrary to global modal parameters such as eigenfrequencies, inherently provides structural information on a local level. A common approach is to exploit that a damage will introduce mode shape discontinuities, albeit not always directly visible ones, which can be captured

by use of signal processing techniques, e.g. continuous wavelet transformation (CWT). Namely CWT has been employed extensively for localizing structural damages in both simple beam- and plate-like systems, see, e.g., [9, 10, 11], and more complex structures such as wind turbine blades [8, 12]. However, by being based on distinguishing damage-induced discontinuities from other signal irregularities, an intrinsic deficiency of the aforementioned CWT-based methods is the rather low robustness towards measurement noise. To treat this issue, a method in which wavelet-transformed mode shapes are processed by use of the discrete Teager-Kaiser energy operator (DTKEO) is proposed in [13]. Here, it is shown, on the basis of analytical and experimental work with different beams, that addition of the DTKEO significantly reduces the sensitivity towards noise.

Compared to the method documented in [13], the method proposed in the present paper constitutes a generalization of the applied signal processing plus an extension by means of outlier analysis to yield the final discrimination between undamaged and damaged areas. As such, the proposed method is composed of three steps; first, a filtered mode shape derivative is obtained of a spatial mode shape signal through CWT, and subsequently a generalized discrete Teager-Kaiser energy operator (GDTKEO) is applied to this derivative to form an energy-processed signal in which the damage-induced discontinuities are magnified. Finally, a statistical evaluation scheme based on T^2-statistics is applied to principal components of these energy-processed, filtered mode shape derivatives in order to label the structures as healthy or damaged at each sensor location/measurement point. To test the applicability of the method, and the potential degree of improvement compared to the method proposed in [13], a free-vibrating, analytical Euler-Bernoulli beam under noisy conditions is analysed.

2. Damage localization method

2.1. CWT

The spatial mode shape signal, $f(x) \in \mathbf{L}^2(\mathbb{R})$, is obtained as a signal-processed version of the original mode shape, $\mathbf{u}$. The signal processing consists of signal expansion in order to remove boundary distortions (resulting in $\mathbf{u} \rightarrow f$). Typically, when dealing with a sparse number of measurement points in, e.g., experiments, an interpolation scheme should also be applied to smooth the mode shape signal and hereby remove artificial discontinuities. However, since analytically derived mode shapes are utilized in this article, the smoothing scheme is omitted.

Based on the spatial mode shape signal, $f(x) \in \mathbf{L}^2(\mathbb{R})$, and the wavelet function, $\gamma(x) \in \mathbf{L}^2(\mathbb{R})$, the CWT is defined as

$$Wf(a,b) = a^{-\frac{1}{2}} \int_{\mathbb{R}} f(x)\gamma^*\Big(a^{-1}\big(x-b\big)\Big)\mathrm{d}x, \tag{1}$$

where $a > 0$ and $b \in \mathbb{R}$ are wavelet scales and positions, respectively. Evidently, the CWT is obtained as the inner product of $f(x)$ and the complex conjugated, indicated with the superscript *, of the so-called wavelet family, which consists of functions constructed from dilations and translations of γ.

The effectiveness of the CWT as a signal discontinuity scanner highly depends on the employed wavelet type; in particular, the amount of vanishing moments, m. Assume $k \in \mathbb{N}^+$, then

$$\forall k < m : \int_{\mathbb{R}} \gamma(x)x^k\mathrm{d}x = 0, \tag{2}$$

which states that a wavelet with m vanishing moments is blind to polynomial trends up to degree $m-1$. Equivalently, when analyzing a spatial mode shape signal with a wavelet with m vanishing moments, a filtered m-derivative of the mode shape is obtained. This becomes evident by realizing that the expression in equation (1) also can be seen as the convolution of f with a scaled, flipped, and conjugated wavelet, thus

$$\exists\theta(x) = \int_{\mathbb{R}} \gamma(x)\mathrm{d}^m x \ni Wf(a,b) = \int_{\mathbb{R}} f(x)\gamma_a^\times(b-x)\mathrm{d}x = \Big(f * \frac{\mathrm{d}^m}{\mathrm{d}x^m}\theta_a^\times\Big)\Big(b\Big) = \Big(\frac{\mathrm{d}^m}{\mathrm{d}x^m}f * \theta_a^\times\Big)\Big(b\Big). \tag{3}$$

This emphasises the importance of choosing a wavelet with a certain minimum of vanishing moments when searching for discontinuities in a signal. Correspondingly, there is also a certain maximum for the proper amount of vanishing moments due to, i.a., magnification of signal noise and adverse border distortions. Clearly, the optimal choice of wavelet strongly depends on signal characteristics such as mode shape type and noise conditions and should therefore be drawn based on these. This is treated further in subsection 3.2.

As stated in section 1, CWTs have previously exhibited damage localization potential. However, as noise is added to the signal, this potential is significantly reduced since the discrimination between noise- and damage-induced CWT peaks becomes troublesome, especially at the lower wavelet scales. For the higher scales, at which noise is better filtered, the low spatial frequency reduces the potential for capturing damage-induced signal discontinuities, thus emphasising the need for further enhancement of these.

2.2. GDTKEO

Since the DTKEO was proposed, originally as a signal energy estimator [14], it has been utilized extensively in speech processing [15], image processing [16], and pattern recognition [17]. Recently, the DTKEO has been adopted to the field of damage identification; as in [18], where it is included in a general damage detection algorithm, and, as mentioned in section 1, in [13], where it is applied to wavelet-transformed mode shapes for damage localization in beams, without any statistical procedure for discriminating between undamaged and damaged areas.

With the notation utilized in the present paper, the DTKEO of a wavelet-transformed mode shape signal at scale a and spatial location i can be found as

$$\psi_{a,i} = Wf_{a,i}^2 - Wf_{a,i-1}Wf_{a,i+1}. \tag{4}$$

In order to enhance the performance of the DTKEO as a signal discontinuity magnifier, it is expanded intuitively by means of a lag parameter, κ, hence yielding the GDTKEO

$$\Psi_{a,i} = Wf_{a,i}^2 - Wf_{a,i-\kappa}Wf_{a,i+\kappa}, \tag{5}$$

i.e. $\Psi_a = \psi_a$ if $\kappa = 1$. As can be realized from equation (5), the lag parameter serves directly to alleviate the adverse noise effects, in analogy to the approach explored for deriving pseudo-modal curvatures through Laplacian operators in [19]. Generally, κ should be chosen on the basis of signal characteristics such as number of measurement points, i.e. signal length, and noise conditions. In subsection 3.2, a simple, yet very effective, method for selecting κ is proposed.

2.3. Outlier analysis

In order to evaluate whether the localized mode shape discontinuities are in fact damage-induced, outlier analysis is conducted by calculating the statistical distance, based on the T^2-statistic, between the signal-processed mode shapes from the present state and similar ones from the healthy state.

Outlier analysis is conducted for each signal band located at a sensor/measurement point, j, such

$$T_j^2 = |\Psi_j|^T P_j \Sigma_j^{-1} P_j^T |\Psi_j| \tag{6}$$

where P_j and Σ_j contain, respectively, the selected principal components (i.e., eigenvectors) and eigenvalues of the covariance matrix of

$$Z_j = \begin{bmatrix} \Psi_{j,\mathrm{train}(1)}^T \\ \vdots \\ \Psi_{j,\mathrm{train}(S)}^T \end{bmatrix}. \tag{7}$$

Evidently, Z_j is a training matrix based on S signal bands at sensor/measurement point j from the baseline, i.e. healthy, state. A signal band at sensor/measurement point j for the current state is then tested on the basis of the following hypothesis:

$$\left.\begin{array}{l} H_{0,j} : T_j^2 \leq \vartheta_j \\ H_{1,j} : T_j^2 > \vartheta_j \end{array}\right\} \tag{8}$$

in which the null hypothesis, $H_{0,j}$, designates that no anomalies are present at the jth sensor/measurement point, whereas the alternative hypothesis, $H_{1,j}$, declares the structure damaged at sensor/measurement point j. The threshold, ϑ_j, is found through the training data. Here, a T^2-statistic between each row in Z_j and the remaining $S-1$ rows is calculated, and subsequently the S T^2-statistics are sorted in an ascending order. Finally, ϑ_j is then chosen as the value exceeded by 1 %.

3. Application example: Analytical beam model

3.1. Cracked Euler-Bernoulli beam

The application example is based on the beam model depicted in figure 1a, which is treated analytically. The beam has a length of L, cross-sectional dimensions of $v = d = 0.03L$, and is assigned an isotropic material model with a Young's modulus, E, corresponding to construction steel, i.e. $E = 200$ GPa. A structural damage with height $s = 0.15d$ is introduced as a crack at location $x/L = 0.4$.

The beam is treated analytically through Euler-Bernoulli beam theory, such transverse vibrations are governed only by the bending deformations. Assuming that the effect of the crack is apparent only in its area, the crack can be modelled as a linear rotational spring with stiffness [20]

$$K_R = \frac{vEI}{6\pi dF(\zeta)}, \tag{9}$$

where EI is the flexural stiffness, while

$$F(\zeta) = 1.86\zeta^2 - 3.95\zeta^3 + 16.37\zeta^4 + 37.22\zeta^5 + 76.81\zeta^6 + 126.9\zeta^7 + 172.5\zeta^8 - 144\zeta^9 + 66.6\zeta^{10} \tag{10}$$

is a dimensionless local compliance function, see e.g. [20], with the independent variable $\zeta = s/d$.

As seen in figure 1b, the spring divides the beam into two separate segments. The transverse motion of each beam segment, $w_i(x)$, is described spatially by the dimensionless governing equation

$$w_i''''(X) - \lambda^4 w_i(X) = 0, \quad i = 1,2, \tag{11}$$

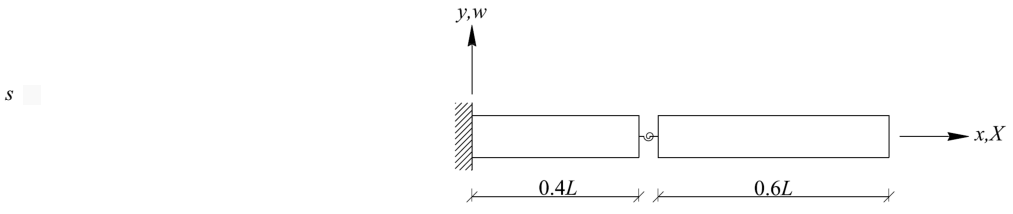

(a) **(b)**

Figure 1. Cracked cantilevered beam. (a) General beam model. (b) Equivalent beam-spring model.

in which $X = x/L$, $w_i''''(X) = \mathrm{d}^4 w_i(X)/\mathrm{d}X^4$, and $\lambda^4 = \omega^2 AL^4\rho/EI$, with ω, A, I, and ρ being the eigenfrequency, the cross-sectional area, the cross-sectional moment of inertia, and the mass density.

Solving equation (11) yields

$$w_i(X) = c_{1,i}\cos(\lambda X) + c_{2,i}\sin(\lambda X) + c_{3,i}\cosh(\lambda X) + c_{4,i}\sinh(\lambda X), \quad i = 1,2, \tag{12}$$

where the constants of integration are found by applying the boundary conditions of the cantilevered beam, i.e.

$$w_1(0) = 0 \quad \wedge \quad w_1'(0) = 0 \quad \wedge \quad w_2''(1) = 0 \quad \wedge \quad w_2'''(1) = 0 = 0, \tag{13}$$

plus the following compatibility conditions in the crack area ($X = X_c$):

$$w_1(X_c) = w_2(X_c) \ \wedge \ K_R\big(w_1'(X_c) - w_2'(X_c)\big) = -EIw_1''(X_c) \ \wedge \ w_1''(X_c) = w_2''(X_c) \ \wedge \ w_1'''(X_c) = w_2'''(X_c). \tag{14}$$

When substituting equation (12) into equations (13) and (14), the characteristic equation is obtained. From here, the eigenfrequencies and subsequently the constants of integration are derived and substituted into equation (12) to yield the mode shapes.

3.2. Damage localization

To demonstrate the applicability and robustness of the proposed method, 300 noise-contaminated (corresponding to a signal-to-noise ratio (SNR) of 65 dB) editions of both the first undamaged (i.e., $K_r = \infty$) bending mode shape and the first damaged bending mode shape are analyzed. 200 of the signal-processed mode shapes from the undamaged state have been randomly chosen to constitute the trained statistical baseline model against which the remaining 100 undamaged signal-processed mode shapes and the 300 damaged signal-processed mode shapes are tested.

3.2.1. CWT settings. When referring to equation (1), it is evident that the CWT is an infinite integral transformation, thus boundary distortions will be introduced when analysing the discrete mode shape signal. In order to reduce these adverse distortions, the mode shape signal is expanded, i.e. $\mathbf{u} \to f$, in accordance with the isomorphism approach [21].

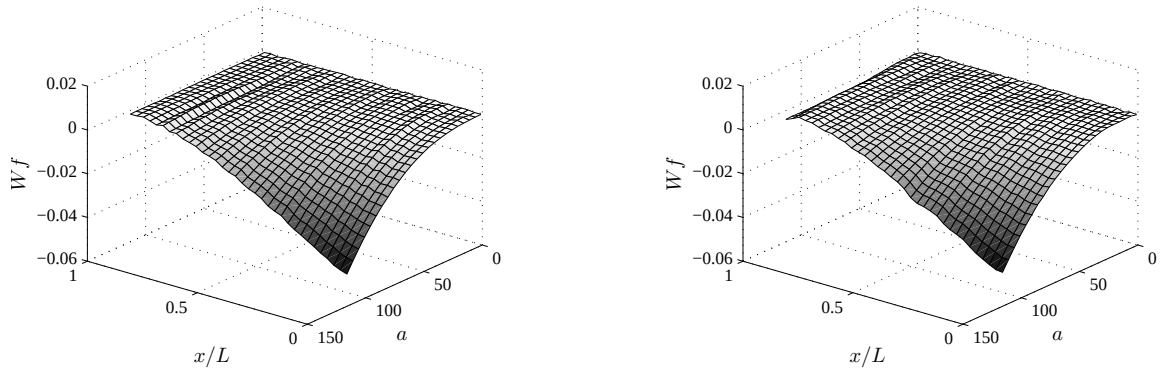

Figure 2. CWT of noise-contaminated (65 dB) first bending mode shape. (a) Undamaged state. (b) Damaged state (crack at $x/L = 0.4$).

In the choice of wavelet type, a crucial parameter is the number of vanishing moments, cf. equation (2). A wavelet with m vanishing moments is blind to polynomials up to order $m-1$, hence implying that a wavelet with a minimum of four vanishing moments would, theoretically, provide the best results when analysing the first bending mode shape. However, extensive amount of differentiation, recall that the CWT yields pseudo-derivatives, would yield detrimental magnification of the border distortions, even when applying the isomorphism approach. Consequently, it is chosen to use a second-order Gaussian wavelet as this has been found to provide a suitable tradeoff between discontinuity enhancement and border distortion magnification. In figure 2, CWTs of noise-contaminated editions of the first bending mode shape of the undamaged beam and the damaged one are presented for the wavelet scale interval $a \in [1,120]$.

3.2.2. GDTKEO settings. As briefly mentioned in subsection 2.2, the lag parameter, κ, serves to alleviate noise contributions. To determine an optimal value of κ, a simple approach based on the root-mean-square (RMS) is proposed. The plot in figure 3a illustrates the principle; the mean of the CWTs (at maximum wavelet scale) from the training state is signal-processed by means of the GDTKEO with different κ values. Then, the RMS is calculated for each of the derived $\Psi_a|_{a=120}$ signals, as plotted in figure 3a, and $\kappa = 342$ is chosen as the value at which the local minimum occurs. By using this setting for the GDTKEO and applying it to the wavelet transforms seen in figure 2, the results presented in figures 3b and 3c are obtained. Clearly, the damaged-induced discontinuity is located along with other irregularities, hence emphasising the need for statistical discrimination.

3.2.3. Outlier analysis. It is chosen to present outlier analysis results for four measurement points/sensor locations, namely $x/L = 0.04$, $x/L = 0.4$ (damage location), $x/L = 0.5$, and $x/L = 0.8$. Here, the statistical model for each location, composed of P_j and Σ_j, have been trained by means of

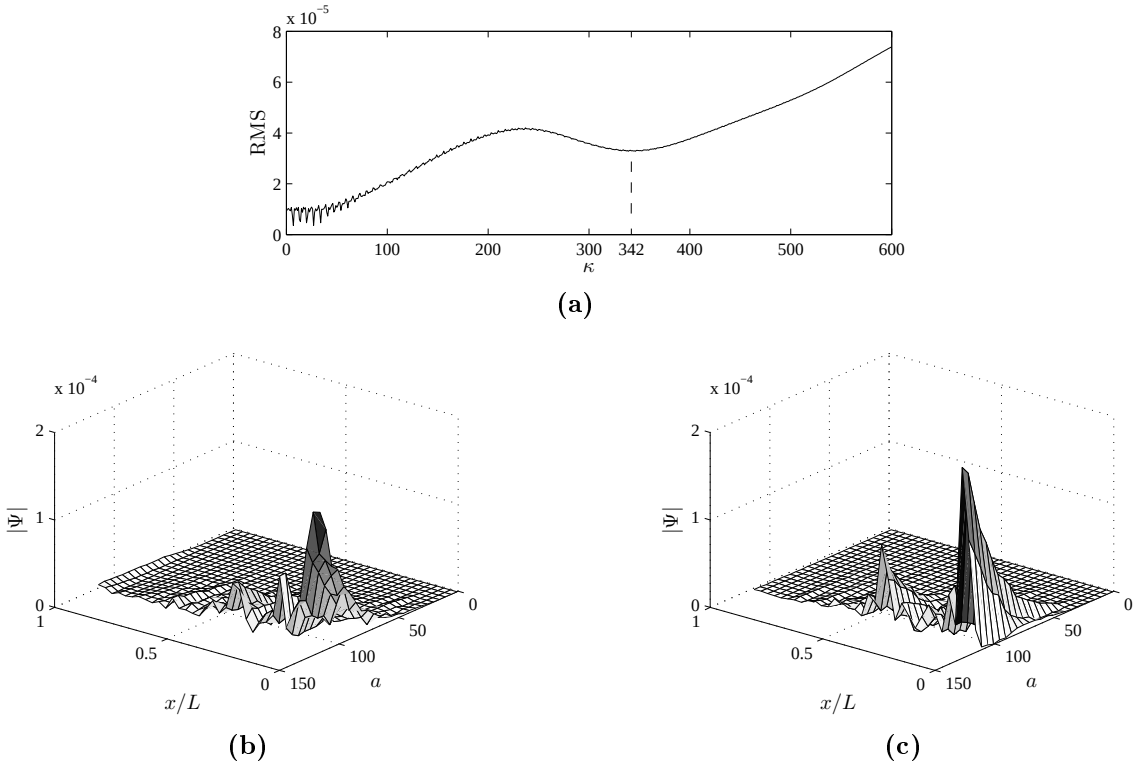

Figure 3. GDTKEO applied to CWT of noise-contaminated (65 dB) first bending mode shape. (a) Selection of κ. (b) Undamaged state for $\kappa = 342$. (c) Damaged state for $\kappa = 342$ (crack at $x/L = 0.4$).

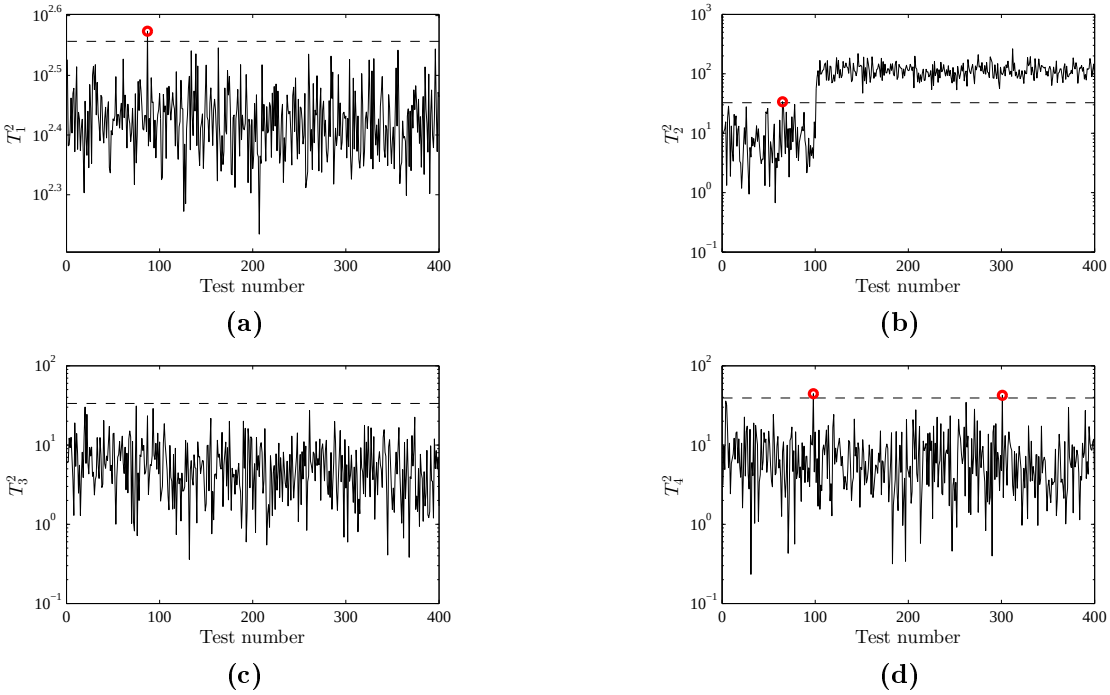

Figure 4. T_j^2-statistics on the basis of $|\Psi|$ ($\kappa = 342$) for undamaged (test number 1-100) and damaged (test number 101-400) states. (a) $x/L = 0.04$. (b) $x/L = 0.4$ (damage location). (c) $x/L = 0.5$. (d) $x/L = 0.8$. The dashed, horizontal lines mark the thresholds and the red circles designate type I errors.

the relevant signal bands from the chosen 200 undamaged signals. It is found, for all four locations, that the two first principal directions contain above 90 % of the variance, and therefore it is chosen only to use these two, thus $P_j \in \mathbb{R}^{200\times 2}$ and $\Sigma_j \in \mathbb{R}^{2\times 2}$. The corresponding thresholds are computed on the basis of the relevant bands from the 200 randomly chosen signal-processed mode shapes from the undamaged state, i.e. $Z_j \in \mathbb{R}^{200\times 120}$.

With the training and threshold computation completed, the testing is conducted. First, the relevant bands from the remaining 100 undamaged signal-processed mode shapes are tested, followed by the corresponding bands from 300 damaged counterparts. In figure 4, the results are presented. Evidently, the data from the healthy configuration, i.e. test number 1-100, are generally classified as inliers. Only a few type I errors, i.e. false outlier classification, are obtained. This is, however, to some extent expectable due to the probabilistic nature of the threshold computation. For test number 101-400, where the beam is damaged at $x/L = 0.4$, the signal-processed mode shape bands at $x/L = 0.4$ are all classified correctly as outliers, see figure 4b. For the three remaining locations, the signal-processed mode shape bands are generally classified as inliers, meaning that the damage localization method yields unambiguous localization of the crack.

As stated previously, the GDTKEO used to obtain the results presented in figure 4 is assigned a lag parameter of $\kappa = 342$. If $\kappa = 1$, the GDTKEO reduces to the DTKEO implemented in the method proposed in [13]. To demonstrate the improvement obtained by using the GDTKEO with a proper selection of κ, instead of the DTKEO, a damage localization analysis analogous to that conducted in this paper (finalised with the results presented in figure 4) is conducted for $\kappa = 1$. The final outlier analysis results, which are seen in figure 5, clearly illustrate the significant improvement obtained by implementing the GDTKEO with a proper κ.

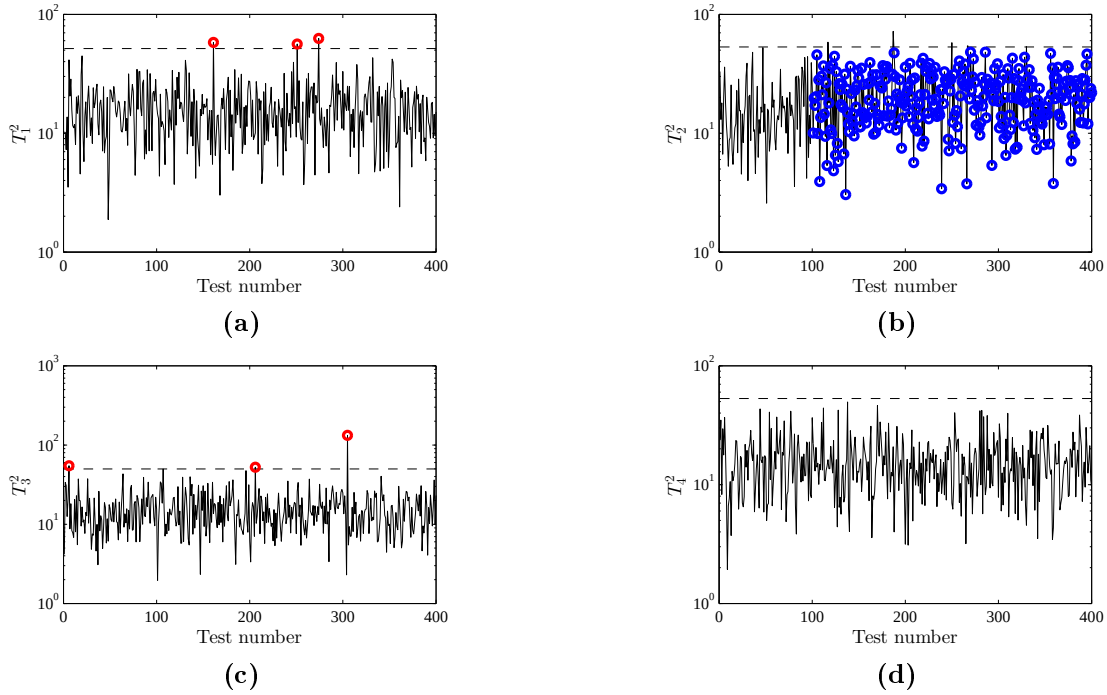

Figure 5. T_j^2-statistics on the basis of $|\psi|$ for undamaged (test number 1-100) and damaged (test number 101-400) states. (a) $x/L = 0.04$. (b) $x/L = 0.4$ (damage location). (c) $x/L = 0.5$. (d) $x/L = 0.8$. The dashed, horizontal lines mark the thresholds and the red and blue circles designate type I and II errors.

4. Conclusion

The present paper documents a proposed damage localization method whose principle is to statistically interrogate changes in signal-processed mode shapes with respect to localization of a damage. As such, the method lacks the need for measuring the excitation input and is completely independent of numerical models.

The applicability of the method has been demonstrated in the context of analytical work with a free-vibrating Euler-Bernoulli beam. Here, 300 noise-contaminated (SNR = 65 dB) editions of the first bending mode shape of the undamaged state and 300 noise-contaminated editions of a damaged state have been signal-processed by means of CWT and subsequent application of a GDTKEO. 200 of the signal-processed mode shapes from the undamaged state have been randomly chosen for training of the statistical baseline model, against which the remaining 100 signal-processed mode shapes from the undamaged state and the 300 signal-processed mode shapes from the damaged state have been tested. Hereby, it is found for the damaged state that the T^2-statistics derived for the signal bands at the damage location are consistently labeled as outliers, whereas the T^2-statistics derived for the remaining locations are classified correctly as inliers (except for a single case). For the undamaged state, only three T^2-statistics are falsely classified as outliers, thus the crack can be unambiguously localized.

References

[1] Salawu O S 1997 *Engineering Structures* **19**(9) 718–723
[2] Doebling S W, Farrar C R, Prime M B and Shevitz D W 1998 *The Shock Vibration Digest* **30** 91–105
[3] Farrar C R, Doebling S W and Nix D A 2001 *Philosophical Transactions of the Royal Society of London A: Mathematical, Physical and Engineering Sciences* **359**(1778) 131–149
[4] Fan W and Qiao P 2011 *Structural Health Monitoring* **10**(1) 83–111
[5] Larsen G C, Berring P, Tcherniak D, Nielsen P H and Branner K 2014 *Proceedings of 7th European Workshop on Structural Health Monitoring*

[6] Creed S G 1987 Assessment of large engineering structures using data collected during in-service loading *Structural Assessment: The Use of Full and Large Scale Testing* ed Garas F K, Clarke J L and Armer G S T (Butterworth-Heinemann) pp 55–62
[7] Aktan A E, Lee K L, Chuntavan C and Aksel T 2001 *Philosophical Transactions of the Royal Society of London A: Mathematical, Physical and Engineering Sciences* **359**(1778) 131–149
[8] Ulriksen M D, Tcherniak D, Kirkegaard P H and Damkilde L 2014 *Proceedings of 7th European Workshop on Structural Health Monitoring*
[9] Douka E, Loutridis S and Trochidis A 2003 *International Journal of Solids and Structures* **40**(13-14) 3557–3569
[10] Loutridis S, Douka E, Hadjileontiadis L J and Trochidis A 2005 *Engineering Structures* **27**(9) 1327–1338
[11] Rucka M and Wilde K 2006 *Journal of Sound and Vibration* **297**(3-5) 536–550
[12] Doliński L and Krawczuk M 2009 *Journal of Physics: Conference Series* **181**(1) 012086
[13] Cao M, Xu W, Ostachowicz W and Su Z 2014 *Journal of Sound and Vibration* **333**(6) 1543–1553
[14] Kaiser J F 1990 *Proceedings of 1990 International Conference on Acoustics, Speech, and Signal Processing* 381–384
[15] Maragos P, Quatieri T F and Kaiser J F 1991 *Proceedings of 1991 International Conference on Acoustics, Speech, and Signal Processing* 421–424
[16] Maragos P and Bovik A C 1995 *Journal of the Optical Society of America A* **12**(9) 1867–1876
[17] Cexus J C and Boudraa A O 2007 *International Journal of Electrical, Robotics, Electronics and Communications Engineering* **1**(2) 321–324
[18] Antoniadou I and Worden K 2014 *Proceedings of 7th European Workshop on Structural Health Monitoring*
[19] Cao M and Qiao P 2009 *Mechanical Systems and Signal Processing* **23**(4) 1223–1242
[20] Dimarogonas A D 1996 *Engineering Fracture Mechanics* **55**(5) 831–857
[21] Messina A 2008 *International Journal of Solids and Structures* **45**(14-15) 4068–4097